Analysis of KIT Mutations in Sporadic and Familial Gastrointestinal Stromal Tumors: Therapeutic Implications through Protein Modeling

Chi Tarn,[1] Erin Merkel,[1] Adrian A. Canutescu,[2] Wei Shen,[1] Yuliya Skorobogatko,[1] Martin J. Heslin,[4] Burton Eisenberg,[5] Ruth Birbe,[3] Arthur Patchefsky,[3] Roland Dunbrack,[2] J. Pablo Arnoletti,[4] Margaret von Mehren,[1] and Andrew K. Godwin[1]

Abstract

Purpose: Gastrointestinal stromal tumors (GIST) are characterized by expressing a gain-of-function mutation in *KIT*, and to a lesser extent, *PDGFR*. Imatinib mesylate, a tyrosine kinase inhibitor, has activity against GISTs that contain oncogenic mutations of KIT. In this study, *KIT* and *PDGFRα* mutation status was analyzed and protein modeling approaches were used to assess the potential effect of *KIT* mutations in response to imatinib therapy.

Experimental Design: Genomic DNA was isolated from GIST tumors. Exons 9, 11, 13, and 17 of c-*KIT* and exons 12, 14, and 18 of *PDGFRα* were evaluated for oncogenic mutations. Protein modeling was used to assess mutations within the juxtamembrane region and the kinase domain of KIT.

Results: Mutations in *KIT* exons 9, 11, and 13 were identified in GISTs with the majority of changes involving the juxtamembrane region of KIT. Molecular modeling indicates that mutations in this region result in disruption of the KIT autoinhibited conformation, and lead to gain-of-function activation of the kinase. Furthermore, a novel germ-line mutation in *KIT* was identified that is associated with an autosomal dominant predisposition to the development of GIST.

Conclusions: We have used protein modeling and structural analyses to elucidate why patients with GIST tumors containing exon 11 mutations are the most responsive to imatinib mesylate treatment. Importantly, mutations detected in this exon and others displayed constitutive activation of KIT. Furthermore, we have found tumors that are both *KIT* and *PDGFRα* mutation negative, suggesting that additional, yet unidentified, abnormalities may contribute to GIST tumorigenesis.

Gastrointestinal stromal tumors (GIST) are the most common mesenchymal tumors of the digestive tract. Mazur and Clark (1) originally described these tumors in 1983, noting they contained smooth muscle and neural elements. Prior to this, GIST tumors were often classified as leiomyosarcomas or leiomyoblastomas. They are believed to arise from the interstitial cells of Cajal (2), the pacemaker cells of the gut, or from interstitial mesenchymal precursor stem cells (3) that also have the potential of giving rise to cells in the omentum and peritoneal surfaces. More recently, it has been recognized that these tumors express KIT also known as CD117 (4).

KIT, a 145-kDa transmembrane glycoprotein, is the normal cellular homologue of the viral oncoprotein v-Kit (5, 6). It is a member of the receptor tyrosine kinase subclass III family that includes receptors for platelet-derived growth factor (PDGF), macrophage-colony stimulating factor, and flt3 (7–11). These kinases have an extracellular domain containing five immunoglobulin-like domains, a single transmembrane domain, and a cytoplasmic domain containing a split kinase domain and hydrophilic kinase insert sequence (12). The juxtamembrane and kinase domains of these receptors are strongly conserved (13). KIT is normally expressed by hematopoietic progenitor cells, mast cells, germ cells, interstitial cells of Cajal, and also by certain human tumors (14–18). Studies of KIT in mouse models have shown that the protein is essential for hematopoiesis, melanogenesis, gametogenesis, mast cell growth, and the differentiation and development of interstitial cells of Cajal (19–22).

The reclassification of GIST based on the expression of KIT was complemented by the understanding that in the majority of these tumors the *KIT* gene is mutated and constitutively activated, leading to disregulated growth (23). A minority of GISTs have a constitutively activated PDGF receptor α (PDGFRα) as the disregulated growth initiator rather than KIT (24, 25).

The treatment of GIST has been revolutionized by the development of imatinib mesylate, a tyrosine kinase inhibitor

Authors' Affiliations: Departments of [1]Medical Oncology, [2]Basic Sciences, and [3]Pathology, Fox Case Cancer Center, Philadelphia, Pennsylvania; [4]Department of Surgery, University of Alabama at Birmingham, Alabama; and [5]Norris Cotton Cancer Center, Dartmouth-Hitchcock Medical Center, Lebanon, New Hampshire

Received 12/8/04; revised 2/3/05; accepted 2/18/05.

Grant support: NIH CA106588-01, a supplement to 3 U10 CA21661-27, and Specialized Programs of Research Excellence in Ovarian Cancer grant P50 CA83638 (A.K. Godwin), Tobacco Formula Grant from the Pennsylvania Department of Health, National Research Service Awards postdoctoral fellowship (C. Tarn), Bristol Myers Squibb Undergraduate Summer Research Fellowship (E. Merkel), the GIST Cancer Research Fund, and an appropriation from the Commonwealth of Pennsylvania.

The costs of publication of this article were defrayed in part by the payment of page charges. This article must therefore be hereby marked *advertisement* in accordance with 18 U.S.C. Section 1734 solely to indicate this fact.

Requests for reprints: Andrew K. Godwin, Department of Medical Oncology, Fox Chase Cancer Center, 333 Cottman Avenue, Philadelphia, PA 19111. Phone: 215-728-2205; Fax: 215-728-2741; E-mail: Andrew.Godwin@fccc.edu.

with specificity against ABL, BCR-ABL, KIT, and PDGFR (26–28). Therapy with imatinib mesylate leads to prolonged stable disease and response in greater than 80% of patients with metastatic/recurrent GIST (29). Our understanding of the frequency of KIT and PDGFRα mutations in GIST and their therapeutic prognostic value is evolving. Data to date suggest that metastatic GIST tumors with KIT mutations in exon 11 have the highest response rate and survival (30).

In this article, we report the identification of new *KIT* mutations in sporadic GISTs. We also describe a novel germline mutation in *KIT* that is associated with an autosomal dominant predisposition to the development of GISTs. We have analyzed our data and others' and have illustrated a high frequency of mutations that cluster in the juxtamembrane region of KIT. Through protein structural analyses and molecular modeling, we hypothesize that these mutations lead to dissociation of the juxtamembrane segment from its autoinhibitory conformation and thus to constitutive activation and tumorigenesis. Imatinib mesylate binds to activated KIT, and hence KIT with mutations in the juxtamembrane region are more susceptible than wild-type to imatinib mesylate therapy.

Materials and Methods

Clinical gastrointestinal stromal tumor samples. Tumor specimens used in this study were collected following NIH guidelines and protocols approved by the Institutional Review Boards of the Fox Chase Cancer Center and University of Alabama at Birmingham. Specimens were obtained from surgically treated GIST patients at Fox Chase Cancer Center and University of Alabama at Birmingham. All the samples were snap-frozen in liquid nitrogen at the time of surgery and kept at −80°C until use. Blood was obtained following informed consent and DNA was isolated from the leukocyte fraction.

DNA extraction and mutational analysis. Genomic DNA isolation was done as follows: frozen tumor samples ~2 mm in diameter were homogenized in 200 μL of lysis buffer [50 mmol/L Tris-HCl (pH 7.5), 150 mmol/L NaCl, 5 mmol/L EDTA (pH 8.0), 0.5% NP40]. After homogenization, genomic DNA was isolated with the use of Easy-DNA kit (Invitrogen, Carlsbad, California) following the instruction of the manufacturer. The purified DNA was resuspended in 50 μL of Tris-EDTA buffer.

KIT and PDGFRα PCR and DNA sequencing. PCR analysis for *KIT* exons 9, 11, 13, and 17 were done in all cases. Each PCR reactions were done in a 50 μL volume containing 100 ng of genomic DNA, 15 μmol/L of each primer, 0.2 mmol/L deoxynucleotide triphosphate, 5 μL of 10× reaction buffer, and 1 unit of AmpliTaq Gold DNA polymerase (Applied Biosystems, Foster City, CA). The KIT primers used were as follows: exon 9, forward: 5-CCTAGAGTAAGCCAGGGCTTT-3′ and reverse: 5-GACAGAGCCTAAACATCCCCT-3′ (278 bp); exon 11, forward: 5-CTCTCCAGAGTGCTCTAATGA-3′ and reverse: 5-AAGGAAGCCACTGGAGTTCCT-3′ (276 bp); exon 13, forward: 5′-CTGCATGCGCTTGACATCAGT-3′ and reverse: 5′-AGGCAGCTTGGACACGGCTT-3′ (195 bp); and exon 17, forward: 5′-GGTTTTCTTTTCTCCTCCAACC-3′ and reverse: 5′-GCAGGACTGTCAAGCAGAGGA-3′ (180 bp). PCR condition was 30 seconds at 94°C, 30 seconds at 52°C, 1 minute at 68°C for 36 cycles, followed by 10-minute extension at 68°C. Primers for PDGFRα exons 12, 14, and 18 were previously published (31), and used with the same PCR condition described above. PCR products were analyzed in 2% agarose gel electrophoresis and purified by PCR purification kit (Qiagen, Valencia, CA). Direct sequencing was carried out from both directions with BigDye Terminator V3.1 cycle sequencing kit on an ABI PRISM 3100 Genetic Analyzer (Applied Biosystems). Samples showing mutation profiles from direct sequencing were further confirmed by subcloning the purified PCR products with the TOPO TA cloning kit (Invitrogen). For each tumor, four to eight clones were analyzed by Miniprep DNA isolation kit (Qiagen), followed by DNA sequencing with an ABI PRISM 3100 Genetic Analyzer. Both wild-type and mutant sequences were detected in all *KIT* mutation–positive tumors.

Immunoblot assays for phospho-KIT and total KIT. Frozen tumor samples ~2 mm in diameter were homogenized in 400 μL of lysis buffers [50 mmol/L Tris (pH 7.5), 150 mmol/L NaCl, 5 mmol/L EDTA (pH 8.0), 1 mmol/L Na_3VO_4, 1 mmol/L NaF, 1 mmol/L phenylmethylsulfonyl fluoride, and 0.5% NP40] containing protease inhibitor cocktail (Roche, Indianapolis, Indiana). The whole cell extract was made by homogenizing tumors in lysis buffer with a tissue homogenizer (Fisher, Pittsburgh, Pennsylvania) for 30 seconds. The whole cell extract was centrifuged at 10,000 × *g* for 5 minutes and the supernatants were collected and quantitated by Bradford method (Bio-Rad, Hercules, California). Fifty micrograms of whole cell extract were electrophoresed and blotted onto Immobilon-P membrane (Millipore, Bedford, MA.). Membranes were incubated with anti–phospho-KIT (1:1,000 dilution) and anti-KIT (1:1,000 dilution) antibodies (Cell Signaling Technologies, Beverly, MA) in TBS/0.5% Tween 20 with 5% bovine serum albumin at 4°C overnight followed by horseradish peroxidase–conjugated secondary antibody at room temperature for 1 hour. Protein bands were detected by Western Lighting Plus chemiluminescence reagent (Roche).

Structural analysis and protein modeling. The X-ray crystallographic structures of KIT (32) in its autoinhibited conformation and with imatinib mesylate bound were downloaded from the Protein Data Bank (entries 1T45 and 1T46, respectively). Molecular modeling of mutant forms of KIT was done with the side-chain prediction program SCWRL (33). Molecular visualization was done with the use of the Chimera software package (34).

Results

KIT mutational analysis and prognosis of gastrointestinal stromal tumor. Recent clinical studies have shown that response to imatinib in GIST patients is dependent on the mutational status of the proto-oncogene c-*KIT* (30, 31). We first evaluated a series of GISTs for mutations in exons 9, 11, 13, and 17 of KIT, and the results were listed in Table 1. Tumors that were negative for KIT mutations were evaluated for mutations in

Table 1. Distribution of c-*KIT* mutations in clinical gastrointestinal stromal tumors (*N* = 25)

Mutation status	No. patients	%
Exon 9	1	4
Insertion	1	
Exon 11	15	60
Deletion	6	
Deletion and insertion	1	
Deletion and substitution	3	
Substitution	5	
Insertion	0	
Exon 13	1	4
Substitution	1	
Exon 17	0	0
No mutations (KIT or PDGFRα)	8	32

NOTE: 60% (15 of 25) of tumors analyzed contain mutation in exon 11. Four percent (1 of 25) has mutation in exons 9 and 13, respectively. We note that there is no mutation detected in exon 17.

PDGFRα because it has been reported that KIT mutation–negative tumors may harbor mutations in PDGFRα (24). In that report, when compared with KIT-positive GISTs, these KIT-negative GISTs are more likely to have epithelioid cell morphology, arise in the omentum/peritoneal surface, and contain PDGFRα oncogenic mutation (24). Among the patients examined in our study, 13 were males and 12 were females, with a median age of 50 years (range, 22-78 years; Table 2). The stomach (10 of 25, 40%) and small bowel (8 of 25, 32%) were the most common sites of primary tumors (Table 2). The median tumor size was 6.9 cm (range, 3.2-32.5 cm). Morphologically, 17 patients had the spindle cell type, 3 had the mixed cell type, and 3 had pure epithelioid tumors. The risk stratification (35, 36) of the GIST (malignant potential based on tumor size and mitotic count) was low in 16% (4 of 25) of the patients and high in 72% (18 of 25) and unavailable in 8% (2 of 25) of the patients. These frequencies did not differ significantly when evaluated in patients with KIT mutation–positive tumors (17% low and 83% high). However, in our study the KIT-negative GISTs primarily have a spindle morphology (Table 2).

Overall, we detected c-*KIT* mutations in 17 of 25 tumors (68%; Table 1). These mutations included in-frame deletions, often coupled with a missense mutation, insertions, and amino acid substitutions. All the *KIT* mutations detected were determined to be heterozygous as a result of sequencing both the PCR products directly and the subcloned PCR products. The majority of the mutations were found in the juxtamembrane region of KIT encoded by exon 11, and involved amino acids 556 to 560 (13 of 15, 87%; Fig. 1A; Table 2). Only two tumors, patients 6 and 14, had mutations in the juxtamembrane region but located outside this cluster, M552_Y553del and D579del, respectively. Two of the other *KIT* mutations fell outside of the juxtamembrane region in exon 9 (patient 17; 1 of 25, 4%) and exon 13 (patient 16; 1 of 25, 4%), and no mutations were found in exon 17 (Table 1). These frequencies are consistent with previous studies, which have found that exon 11

Table 2. Clinical-pathologic features of GISTs with and without c-*KIT* mutations

Case no.	Exon	KIT mutation	Age/ Gender	Site	Size (cm)	Mitosis/no. HPF	Histology	Risk	Follow-up	Response
1	11	1669del24, 1693ins6; K550_W557del, I558L559ins	37/M	Omentum/retrop	8.5	39/50	Epithelioid	High	DOD	PD
2	11	1690del6, 1695G>C; Q556_W557del, K558N	60/F	Stomach	15	49/50	Spindle	High	DOD	NA
3	11	1693del6; W557_558del	72/F	Colon	15	0/50	Spindle	High	NED	SD
4	11	1697T>G; V559G	70/F	Stomach	23	10/50	Spindle	High	NED on obs	NA
5		1697T/A; V559D	57/M	Small bowel	7.2	>200/50	Spindle	High	DOD	NA
6	11	1675del6; M552_Y553del	66/F	Small bowel	3.5	2/50	Mixed	Low	NED	NA
7	11	1696del3; V559del	36/M	Stomach	13.5	NA	Epithelioid	High	DOD	NA
8	11	1687del15; Q556_V560del	63/F	Duodenum	4.5	25/50	NA	High	NED	NA
9	11	1695del3; K558I, V559del	65/M	Distal ileum/rt colon	32.5	NA	Spindle	High	AWD	Progression
10	11	1689del48; Q556H, W557_D572del	52/F	Duodenum	3.6	0/50	Spindle	Low	NED	NA
11	11	1697T>A; V559D	78/M	Stomach	6.9	15/50	Spindle	High	NED	NA
12	11	1697T>A; V559D	69/F	Stomach	16	5/50	NA	High	NED	NA
13	11	1700T>G; V560G	69/M	Stomach	4	20/50	Spindle	High	NED	NA
14	11*	1753del3; D579del	36/F	Stomach	12	15/50	Mixed	High	AWD	SD
15	11	1692G>T, 1693del9; W557C, K558_V560del	65/F	Stomach	12.5	>200/50	Spindle	High	NED	NA
16	13	1946A>G; K642E	63/M	Small bowel	4.9	0/50	Spindle	Low	NED	NA
17	9	1530ins6; A502Y503ins	46/M	Small bowel	6.0	18/50	Spindle	High	DOD	NA
18	Wt	None	53/M	Stomach	5.5	1/50	Epithelioid	High	2 mets at dx	PR
19	Wt	None	49/F	Small bowel	11.5	0/50	Spindle	High	NED	PR
20	Wt	None	51/M	Small bowel	9	0/50	Spindle	High	AWD	PR
21	Wt	None	48/M	Rectum	4.5	12/50	Spindle	High	NED	NA
22	Wt	None	48/M	Small bowel	6.5	136/50	Spindle	High	mets site	NA
23	Wt	None	52/F	Duodenum	4	3/50	Spindle	Low	NED	NA
24	Wt	None	62/M	Stomach	3.2	NA	Spindle/ leiomyoma	NA	NED	NA
25	Wt	None	22/F	Small bowel	6.5	NA	Mixed	NA	DOD	NA

Abbreviations: HPF, high-power field; DOD, dead of disease; NED, no evidence of disease; AWD, alive with disease; PR, partial response; SD, stable disease; NA, not available.

*Mutation found in the germline of patient 14 and her mother diagnosed with GIST.

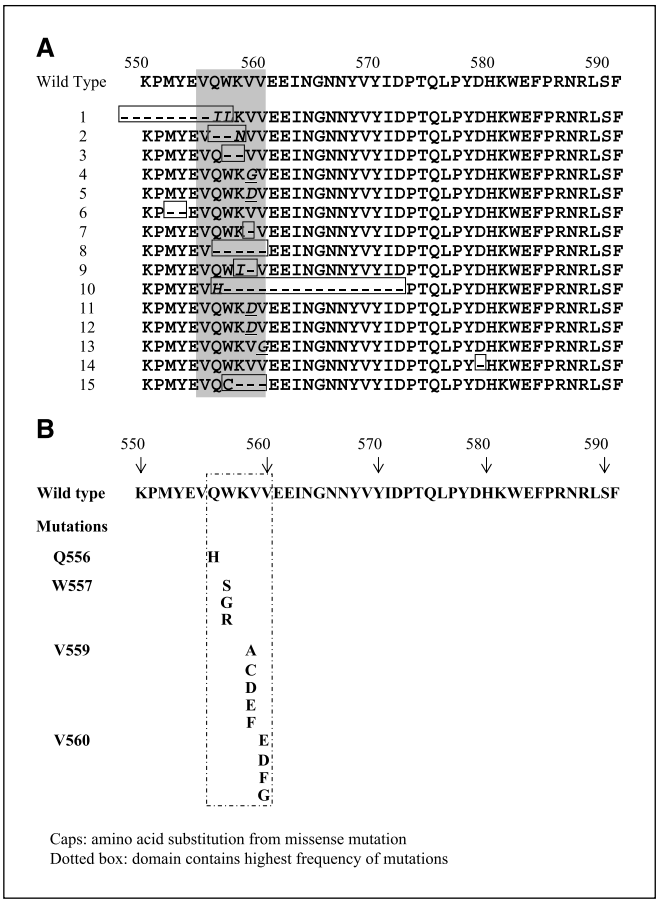

Fig. 1. *KIT* mutations in GISTs. *A*, amino acid sequence of *KIT* exon 11 mutations in clinical GIST biopsies. –, amino acids that are deleted; italicized amino acids, mutations (insertion or deletion) and the corresponding amino acid substitution. Italicized and underscored amino acids, missense mutations and the corresponding amino acid substitution. Shaded box, amino acids 556 to 560 which are altered in the majority of tumors examined. *B*, high frequency of missense mutations in *KIT* exon 11 encoding amino acids 556 to 560. Summary of amino acid substitutions reported by us (in this report) and others (36, 39, 40).

mutations are predominant in GIST, whereas mutations in exon 9, 13, and 17 are rare events in GIST (37, 38). A summary of high-frequency mutations in c-*KIT* exon 11 is listed in Fig. 1B. The high frequency was defined by the rate of mutations in ~428 patients determined from our study and from others (36, 39, 40).

We also showed that the somatic mutations we identified in KIT lead to constitutively activation as determined by immunoblotting for the phosphorylated receptor; a surrogate gauge of kinase activity. Tumors possessing a KIT mutation expressed varying levels of phosphorylated KIT (Fig. 2, *lanes 1-7*; Table 2) as compared with a GIST with no detectable KIT mutation (Fig. 2, *lane 8*; Table 2). Our results suggest that the juxtamembrane region of KIT encoded by exon 11 is mutated in the majority of the GISTs we evaluated, including a familial case of GIST, and results in disruption of the KIT autoinhibited conformation, leading to gain-of-function activation.

PDGFRα mutation analysis. Surprisingly, we failed to detect any mutation in *PDGFRα*, focusing on exons 12, 14, and 18, which have previously been shown to be mutated in a subset of wild-type KIT GISTs (24). However, we did find a silent missense variant in *PDGFR* exon 18 at position 2472C>T (V824V) in GIST DNAs. The *2472C>T* allele was found in 8 of 25 GIST patients (32%). Single nucleotide polymorphism analysis of 96 disease-free individuals (48 men and 48 women) showed that 22% (10 males and 11 females of 96 individuals) carry a *T2472* allele, whereas only 2% (2 of 96) were homozygous for the *T2472* allele. The proportion of samples with TT or Tt was not significantly different between cases and controls ($P = 0.445$; two-sided Fisher's exact test). Overall, these results suggest that 2472C>T in PDGFRα is likely a benign polymorphism and is not significant in the pathogenesis of GIST.

Gastrointestinal stromal tumor–prone kindred. Review of available family history of GIST patients found a GIST family kindred. Patient 14 was diagnosed with GIST at age 37. Her mother was also found to have a GIST the previous year at age 57. In addition, the maternal grandmother was also diagnosed with GIST at age 80 and other third-degree relatives with esophageal and breast cancer (Fig. 3A). Blood was obtained from patient 14 and her mother and a *KIT* mutation, a 3 bp deletion, 1753del3 (leading to deletion of amino acid 579), was found in the germ line of both individuals (Fig. 3B). This same mutation was found in the tumor tissue of patient 14. This germ-line 1753del3 *KIT* mutation resides at the first tyrosine kinase catalytic domain of KIT protein and is a novel germ-line mutation not previously reported. This patient underwent surgical resection of a gastric GIST and was found to have peritoneal metastasis at the time of surgery. The resected tumor displayed central calcification suggesting a slow process of necrosis and cell death. Her disease has had a relatively indolent course and she has stable residual tumors while receiving imatinib treatment.

KIT/imatinib structural analysis. The mutations identified in our clinical study were mapped (Fig. 4A-D) on the crystal structure of the autoinhibited KIT (PDB entry 1T45) and on the structure of activated KIT (PDB entry 1T46; ref. 32). Figure 4A shows the wild-type KIT in its autoinhibited conformation. We modeled each of the mutations listed in Table 1, starting from the autoinhibited experimental structure with the program SCWRL (33). In Fig. 4B we show a model of the V559D mutation from case 13. As shown in Fig. 2 (*lane 6*, *case 13*), this mutation leads to constitutive activation of KIT. The model shows that D559 would extend into the hydrophobic binding site normally occupied by V559. The mutation removes favorable hydrophobic interactions of the side chain of V559 with the side chains of V643, Y646, and V647, and burying of a charge away from solvent into a hydrophobic site. Table 3 lists

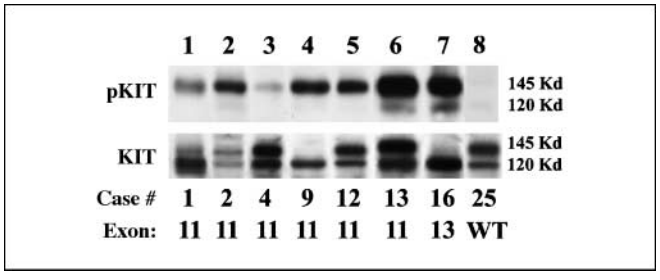

Fig. 2. Immunoblot analysis of KIT and phosphorylated KIT. GIST protein extracts were evaluated for total KIT and phosphorylated receptor as described in Materials and Methods. The case numbers (1, 2, 4, 9, 12, 13, and 16) shown correspond to the mutation listed in Table 2. Both total and phosphorylated KIT are detected in the seven cases shown (*lanes 1-7*). Case 25 (*lane 8*), a GIST with wild-type KIT, expresses total KIT, but lacks the phosphorylated receptor.

the other physical-chemical changes due to mutations seen in GIST patients in the segment 556 to 560 of KIT. Mutations within amino acid residues 556 to 560 are very likely to disrupt the hydrophobic (W557, V559, and V660) or electrostatic (Q556) interactions that favor docking of the hairpin loop between the kinase N and C domains. Disruption of binding of the autoinhibitory region therefore leads to release of the juxtamembrane region and to gain-of-function activation of KIT.

A mutation outside of the segment 556 to 560 was observed in KIT exon 13 from a GIST patient (case 16; Fig. 2, *lane 7*; Table 2). This missense mutation replaces lysine with glutamic acid at position 642. The X-ray structure of KIT shows that the K642 side chain makes hydrogen bonds to the carbonyl

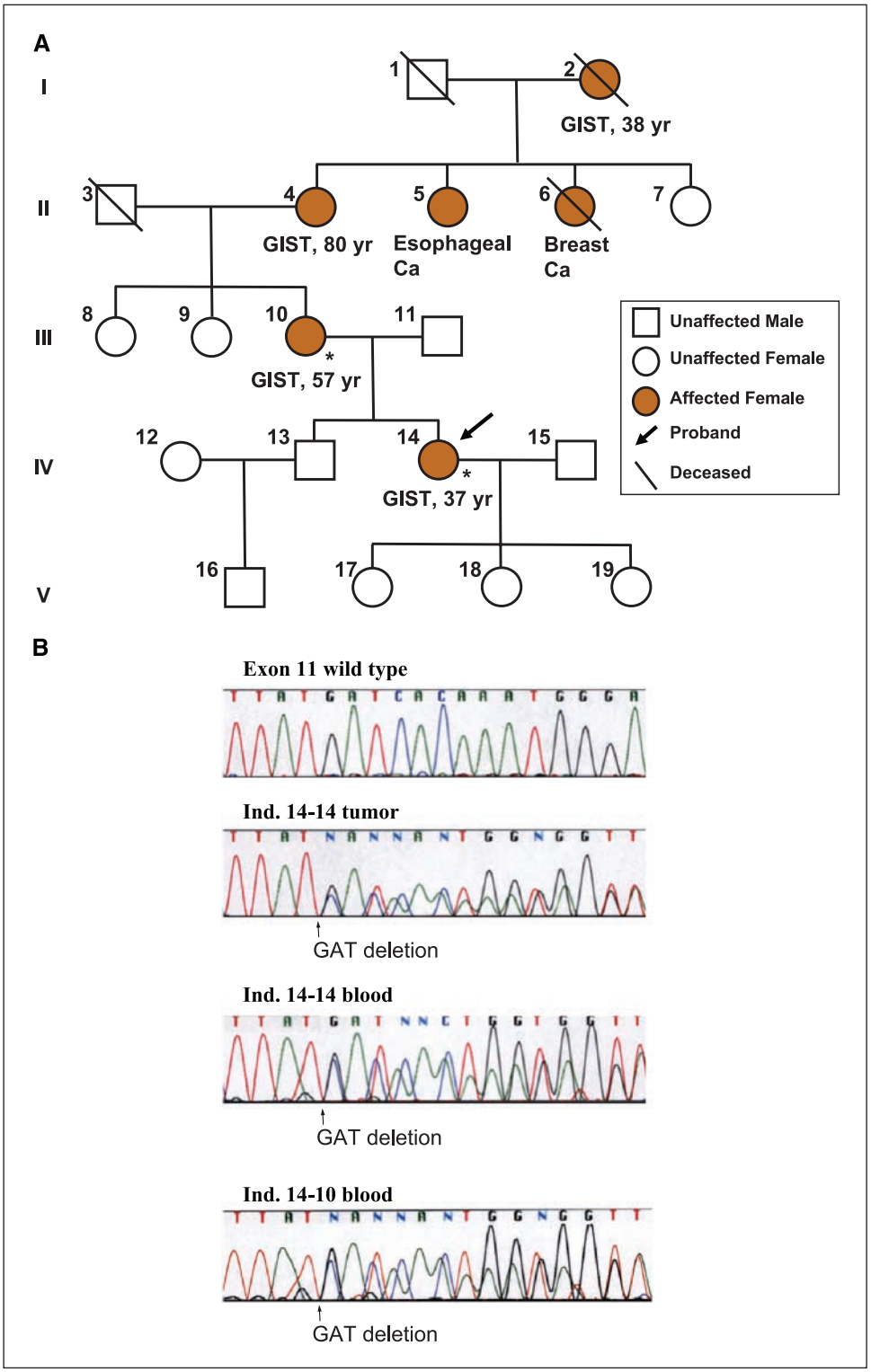

Fig. 3. Familial case of GIST. *A*, family pedigree for individual 14. The age of diagnosis is given when available. *B*, direct sequence traces of germ-line and tumor mutations from the proband, 14-14, and her mother, 14-10.

oxygens of residues T574 and L576, as shown in Fig. 4C. These carbonyl oxygens are only 3.6 Å apart, which would create a large electrostatic repulsion in the absence of the Lys side-chain hydrogen bonds. It is likely that replacing the positively charged Lys side chain with a negatively charged Glu side chain (shown in Fig. 4D) would disrupt the conformation of residues 573 to 577, with potentially long-range consequences on the structure of autoinhibited KIT. These residues follow the autoinhibitory hairpin loop and the K642E mutation may therefore potentially alter the binding of the loop. Interestingly, this patient has high level of phosphorylated KIT (Fig. 2, *lane 7*) but is considered to be at low risk for recurrence (Table 2). Table 3 displays the identified mutations together with the physical-chemical differences between the wild-type and mutant residues in a specific position.

Importantly, none of the mutations in exon 11 seem to be responsible for modifications in the nucleotide binding site and, therefore, mutated KIT should remain responsive to imatinib. Together, the high-frequency mutations within amino acids 556 to 560 and their role in altering KIT structure are consistent with the clinical findings, by which the identified mutations are tumorigenic, but at the same time are associated with a high rate of positive response to imatinib treatment.

Discussion

GISTs are mesenchymal neoplasms of the digestive tract that are typically characterized by *KIT* mutations in exon 9, 11, 13, or 17 resulting in the constitutive activation of the KIT tyrosine kinase in ~90% of GISTs (23). The remaining GISTs have either activating mutations of tyrosine kinase *PDGFRα* or lack any identifiable receptor tyrosine kinase mutations (24).

Imatinib mesylate, a competitive inhibitor of ABL, BCR-ABL, KIT, and PDGFR tyrosine kinases, has been used as a successful therapeutic in GIST patients with metastatic or unresectable disease (41–46). However, imatinib therapy has resulted in few pathologic complete responses and drug resistance is observed with increasing duration of therapy. In addition, response to imatinib varies with different mutations of *KIT* or *PDGFRα*. Heinrich et al. (30) showed that *in vitro* wild-type and all *KIT* mutant isoforms in GIST respond to imatinib. Clinically, however, GIST patients with *KIT* exon 11 mutations (i.e., the juxtamembrane region) are the more sensitive to imatinib as compared with wild-type *KIT*/*PDGFRα* or exon 9 mutations (30, 47, 48).

In this study, we report that 68% of total patients examined possess *KIT* mutation. Among them, 88% (15 of 17 KIT mutation–positive patients) have mutation in exon 11, and 6% (1 of 17) have mutation in either exon 9 or 13. Our results are in general agreement with other reported mutational frequencies for *KIT* exon 11, which ranged from 20% to 92%, depending on the methodology used and sample source (e.g., frozen or paraffin-embedded tissues; refs. 36, 37). We did, however, observe that three of the patients (cases 19, 20, and 21) evaluated displayed partial response to initial administration of imatinib, although they were negative for both *KIT* and *PDGFRα* mutations. Tissue samples from these three patients were obtained following neoadjuvant therapy and potentially had low tumor cellularity in the samples as a result of tumor response to imatinib mesylate therapy. Therefore, care must be taken in selecting viable tumor specimens, particularly after imatinib treatment, for mutational analysis of *KIT* and/or *PDGFRα* as a molecular screening test to predict response to imatinib. Such tests will probably become more widely accepted in the near future as is being considered for the *EGFR* gene in the treatment of non–small-cell lung cancer with gefitinib (49, 50). However, frozen GIST tumors from patients with good clinical data represent a unique opportunity to define a specific molecular profile in relation to clinical response, mutational status, and crystalline structure towards a predictable therapeutic index.

The majority of our tumors stained positive for KIT (data not shown) and contained exon 11 mutations (Tables 1 and 2). Most of the exon 11 mutation patients we detected were considered at "high risk" for disease progression, based on clinical and pathologic criteria (Table 2). The preponderance of high-risk tumors may reflect a selection bias based on samples being obtained from two tertiary-care academic centers and that tumors that were banked tend to be larger. The number of small bowel tumors included in our analysis, which have been reported to have poorer prognosis by some, may also be an explanation for the high numbers of high-risk tumors.

Histologically all tumors examined in this study were primarily of spindle cell or mixed spindle and epithelioid type, with only three patients having an epithelioid histology (Table 2). The distribution of our samples is in agreement with the current knowledge of pathologic features of GISTs (i.e., 70% of cases of GISTs are comprised of spindle cells, 20% of cases are epithelioid cells, and 10% of cases consist of a mixture of the two phenotypes; refs. 36, 51).

Our studies also identified a new germ-line mutation of c-*KIT*, a 3-base in-frame mutation (1753del3) leading to the loss of a single amino acid at position 579 (D579del). Interestingly, this germ-line mutation did not fall in the region of high-frequency mutation of c-*KIT* exon 11 (Fig. 1B). From the family pedigree, four family members, all female, were also reported to have GIST and two additional female relatives were reported to have esophageal and breast cancer, respectively (Fig. 3A). Blood leukocyte DNA from both mother and daughter indicated that the mutation was inherited (Fig. 3B). The extent of other cancers associated with germ-line *KIT* mutations has not been thoroughly evaluated. Anecdotally, we and others have observed a greater frequency of second malignancies in GIST patients than would be expected. The biological significance of this observation is not known at this time.

There are several reports of familial cancer syndromes of GIST tumors (52–56). The first report described a family with multiple GIST, both malignant and benign. These individuals were found to have a *KIT* mutation occurring between the transmembrane and tyrosine kinase domains, both in the tumor and peripheral leukocytes. Other family members were shown to have somatic mutations of KIT (52). Maeyama et al. (53) described a family with cutaneous hyperpigmentation presenting in adolescence followed by the diagnosis of multiple GIST tumors in their 40s. This family was found to have a germ-line mutation in KIT at codon 559 of exon 11 (V559A), which was the same as that found in the GIST. Evaluation of leukocytes from a sibling with hyperpigmentation but no diagnosis of GIST revealed the same mutation, but her two offsprings were without hyperpigmentation or mutation. Other germ-line mutations have been reported in exon 13 with a Lys to Glu substitution (K642E; ref. 54) and in exon 17 with an Asp to Tyr (D820Y) substitution, which lead to gain of function

(55). All four mutations identified in these families (D579del, V559A, K642E, and D820Y) affect the intracellular kinase domain of the *KIT* protein. We also identified a mutation in exon 13 of c-*KIT* but do not have a family history or tissue, but suspect that this maybe a family prone to GIST.

Our studies highlighted that the majority of mutations in the juxtamembrane region of KIT encoded by exon 11 typically involve amino acids 556 to 560 (13 of 15, 87%). Within our series of GIST, we uncovered four missense mutations affecting amino acid 559 (V559D or V559G) and one leading to a substitution at residue 560 (V560D). In total, 11 of the 15 exon 11 mutations altered either or both of residues 559 and 560 (Fig. 1A). Available protein extracts indicated that all of these mutations resulted in expression of a phosphorylated KIT at varying levels (Fig. 2 and data not shown).

Analysis of the X-ray crystallographic structures of autoinhibited and activated KIT reveals a potential mechanism for the activation of KIT through acquired or inherited mutations in the juxtamembrane region and susceptibility of these mutant proteins to inhibition by imatinib. KIT, like many protein kinases, has two states: active and autoinhibited conformations (32). In KIT, as suggested for other Type III receptor phosphotyrosine kinases, the juxtamembrane domain functions as an autoinhibitory domain. In the autoinhibited state, the juxtamembrane region forms a hairpin loop that docks in the interface between the kinase N and C lobes. Consequently, the control helix and the kinase DFG motif undergo a conformational change. In the autoinhibited conformation, Trp557 takes the place occupied by Phe811 in the active conformation, Phe811 being flipped toward the binding site

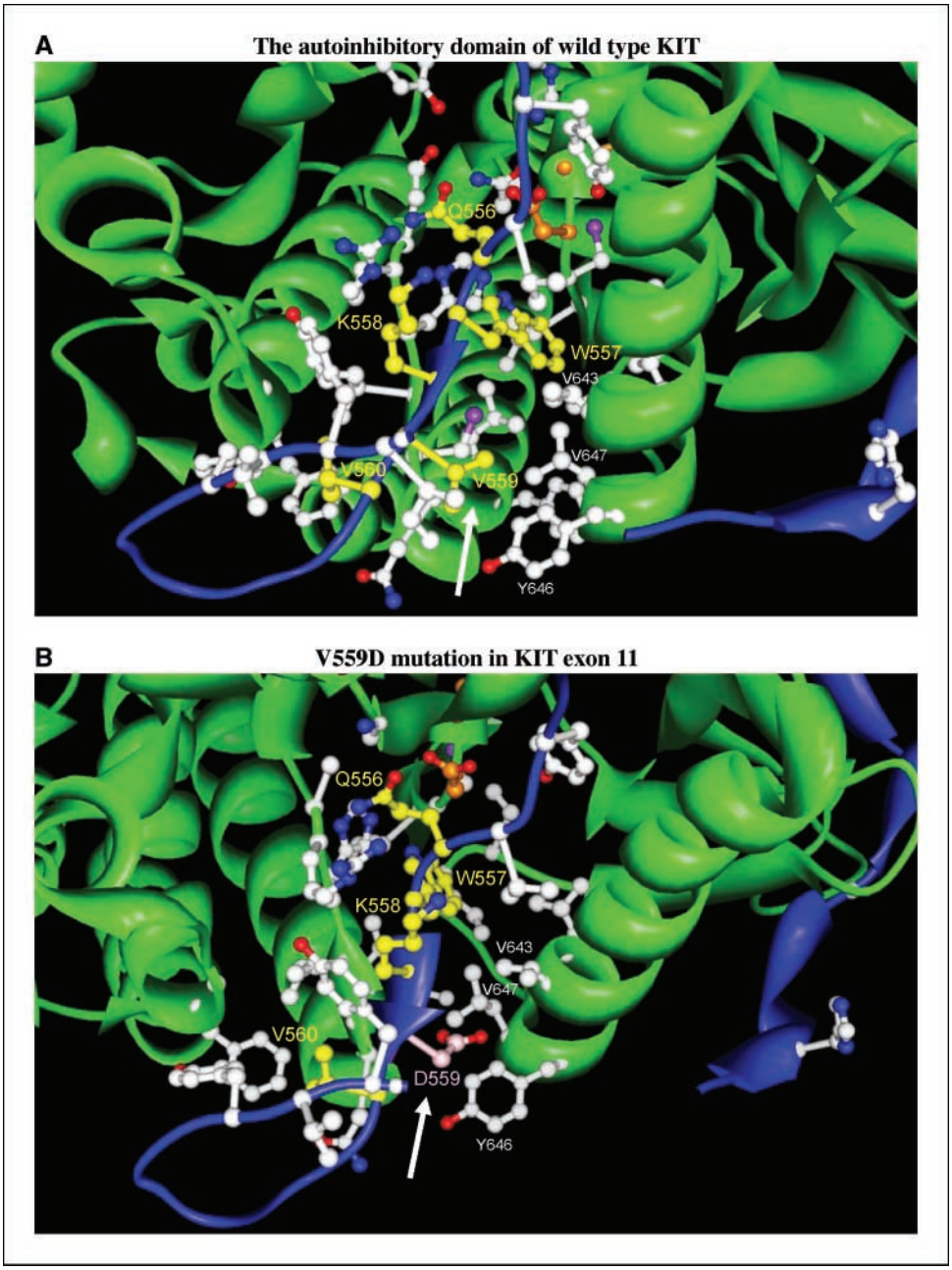

Fig. 4. Structural analysis and protein modeling of KIT mutations. *A*, model of wild-type KIT based on published crystal structure (32). Note that amino acids residues 556 to 560 (*yellow*) are part of the autoinhibitory domain. Arrowhead, wild-type residue V559. *B*, model of V559D, one of the high-frequency mutations in exon 11. Arrowhead, mutant residue D556. Note the conformational change due to this single amino acid mutation.

and preventing nucleotide binding. Furthermore, in the autoinhibited state, the activation loop is switched from an active extended conformation to a folded one, in which it also acts as a pseudosubstrate (32).

The buried part of the inhibitory domain, involved in the interactions with the kinase DFG motif and activation loop, is composed of residues 547 to 565 (Fig. 4A). Experimentally it has been shown by mutational analysis that the juxtamembrane domain, especially residues 557 to 560, has the most important contribution to the interaction between the autoinhibitory domain and the kinase domain (57–59). Particularly, Val559 and Val560 are involved in a hydrophobic packing with Val643, Tyr646, Cys788, and Ile789 (32). Mutations in residues 556 to 560 resulted in destabilization of the autoinhibitory domain due to elimination of favorable hydrophobic interactions, therefore leading to gain-of-function (Fig. 4A and B; Table 3). From our structural analysis, we have compared the conformational change of the autoinhibited structure (wild-type, Fig. 4A) with the V559D mutation (Fig. 4B). It is clearly shown that V559D mutation is unfavorable in maintaining the structure of the autoinhibitory domain. Substitution of a hydrophobic amino acid (V) with a negatively charged residue (D) in this domain is energetically unfavorable. Furthermore, a patient-derived mutation, K642E,

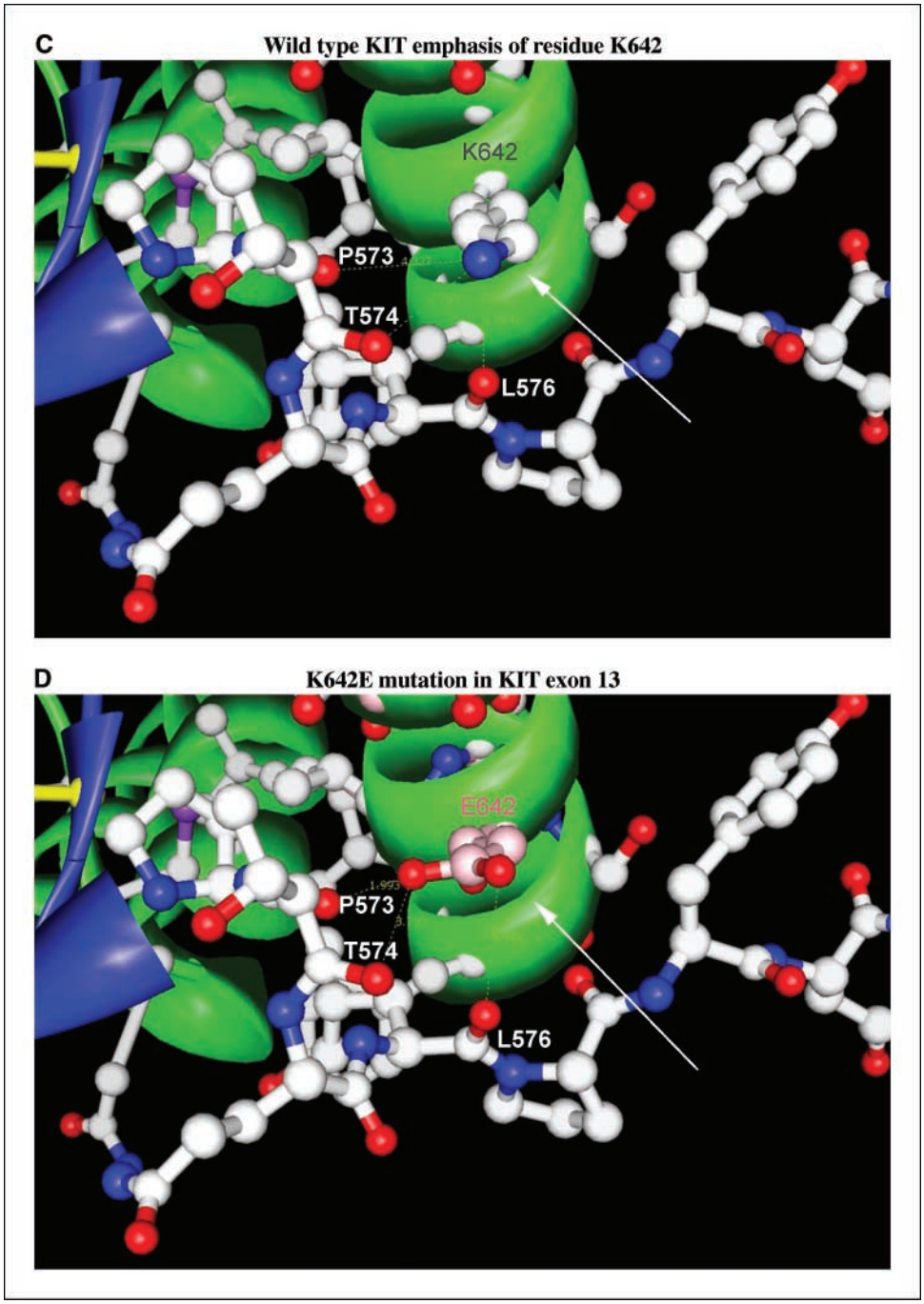

Fig. 4 *continued. C*, model of wild-type KIT with emphasis of residue K642. Arrowhead, wild-type residue K642. *D*, model of E642 mutation in exon 13. Exon 11 (residues 550-591) is highlighted in blue in all figures.

Table 3. Physical-chemical differences between the wild-type and mutant residues from amino acids 556 to 560

Position	Wild-type residue	Physical properties	Mutation	Physical differences
556	Q	Polar uncharged	H	Larger SC, polar
557	W	Large, hydrophobic	S	Smaller SC, polar
			G	No SC
			R	Positively charged
559	V	Small, hydrophobic	A	Smaller SC
			C	Smaller SC, polar
			D	Larger SC, negatively charged
			F	Larger SC
			G	No SC
560	V	Small, hydrophobic	E	Larger SC, negatively charged
			D	Larger SC, negatively charged
			F	Larger SC
			G	No SC

Abbreviation: SC, side chain.

disrupts side-chain/backbone hydrogen bonds to the juxtamembrane segment residues 574 and 576. Whereas this mutation seems less likely to result in complete dissociation of the juxtamembrane segment from its inhibitory conformation, it may destabilize it sufficiently to result in weak activation of the kinase.

Finally, we did not find a mutation in the *PDGFRα* gene in the *KIT*-negative tumors. This finding is surprising given that recent studies have found a high frequency of *PDGFRα* mutations in *KIT*-negative GISTs (24). Although the number of KIT mutation–negative tumors is relatively small ($n = 5$) or if the pretreated patients were truly KIT wild-type ($n = 8$), based on recent studies we would have expected to identify at least one (~30%) PDGFRα mutation in these GISTs. Our findings continue to support the fact that a subset of GIST is likely both *KIT* and *PDGFRα* mutation negative, and that these tumors are typically refractory to imatinib therapy. Furthermore, the expression of phospho-KIT and phospho-PDGFRα in the double-negative mutant GISTs was not detectable via immunoblotting with anti–phospho-KIT or anti–phospho-PDGFRα (data not shown). Together our results indicate that other mechanisms (such as AKT) which are independent of *KIT* and *PDGFRα* mutations may contribute to the activation of signal transduction pathways and tumorigenesis in GIST. In this regard, we found that GISTs were not likely to carry mutations in the p110 subunit of PI3K[6] although it has been found that PI3K gene catalytic domain (PI3KCA) is highly mutated in human cancers (60–63). We did find that many *KIT* and *PDGFRα* mutation–negative tumors we have examined expressed phosphorylated forms of AKT.[6] Lastly, we showed that protein modeling studies can help explain the response to imatinib mesylate based on the site of mutation.

Acknowledgments

We would like to thank the Molecular Modeling Facility, Biostatistics, Tumor Bank, and the Biosample Repository (http://www.fccc.edu/clinicalresearch/BRCF/) Core facilities at Fox Chase Cancer Center for services and specimens.

[6] Y. Skorobogatko and A. Godwin, unpublished data.

References

1. Mazur MT, Clark HB. Gastric stromal tumors. Reappraisal of histogenesis. Am J Surg Pathol 1983; 7:507–19.
2. Sircar K, Hewlett BR, Huizinga JD, Chorneyko K, Berezin I, Riddell RH. Interstitial cells of Cajal as precursors of gastrointestinal stromal tumors. Am J Surg Pathol 1999;23:377–89.
3. Kindblom LG, Remotti HE, Aldenborg F, Meis-Kindblom JM. Gastrointestinal pacemaker cell tumor (GIPACT): gastrointestinal stromal tumors show phenotypic characteristics of the interstitial cells of Cajal. Am J Pathol 1998;152:1259–69.
4. Sarlomo-Rikala M, Kovatich AJ, Barusevicius A, Miettinen M. CD117: a sensitive marker for gastrointestinal stromal tumors that is more specific than CD34. Mod Pathol 1998;11:728–34.
5. Besmer P, Murphy JE, George PC, et al. A new acute transforming feline retrovirus and relationship of its oncogene v-kit with the protein kinase gene family. Nature 1986;320:415–21.
6. Yarden Y, Kuang WJ, Yang-Feng T, et al. Human proto-oncogene c-kit: a new cell surface receptor tyrosine kinase for an unidentified ligand. EMBO J 1987;6: 3341–51.
7. Claesson-Welsh L, Eriksson A, Westermark B, Heldin CH. cDNA cloning and expression of the human A-type platelet-derived growth factor (PDGF) receptor establishes structural similarity to the B-type PDGF receptor. Proc Natl Acad Sci U S A 1989;86: 4917–21.
8. Yarden Y, Escobedo JA, Kuang WJ, et al. Structure of the receptor for platelet-derived growth factor helps define a family of closely related growth factor receptors. Nature 1986;323:226–32.
9. Coussens L, Van Beveren C, Smith D, et al. Structural alteration of viral homologue of receptor proto-oncogene fms at carboxyl terminus. Nature 1986; 320:277–80.
10. Rosnet O, Schiff C, Pebusque MJ, et al. Human FLT3/FLK2 gene: cDNA cloning and expression in hematopoietic cells. Blood 1993;82:1110–9.
11. Small D, Levenstein M, Kim E, et al. STK-1, the human homolog of Flk-2/Flt-3, is selectively expressed in CD34+ human bone marrow cells and is involved in the proliferation of early progenitor/stem cells. Proc Natl Acad Sci U S A 1994;91:459–63.
12. Broudy VC. Stem cell factor and hematopoiesis. Blood 1997;90:1345–64.
13. Rousset D, Agnes F, Lachaume P, Andre C, Galibert F. Molecular evolution of the genes encoding receptor tyrosine kinase with immunoglobulin-like domains. J Mol Evol 1995;41:421–9.
14. Ishikawa K, Komuro T, Hirota S, Kitamura Y. Ultrastructural identification of the c-kit-expressing interstitial cells in the rat stomach: a comparison of control and Ws/Ws mutant rats. Cell Tissue Res 1997; 289:137–43.
15. Russell ES. Hereditary anemias of the mouse: a review for geneticists. Adv Genet 1979;20:357–459.
16. Nocka K, Majumder S, Chabot B, et al. Expression of c-kit gene products in known cellular targets of W mutations in normal and W mutant mice—evidence for an impaired c-kit kinase in mutant mice. Genes Dev 1989;3:816–26.
17. Natali PG, Nicotra MR, Sures I, Mottolese M, Botti C, Ullrich A. Breast cancer is associated with loss of the c-kit oncogene product. Int J Cancer 1992;52:713–7.
18. Turner AM, Zsebo KM, Martin F, Jacobsen FW, Bennett LG, Broudy VC. Nonhematopoietic tumor cell lines express stem cell factor and display c-kit receptors. Blood 1992;80:374–81.
19. Migliaccio G, Migliaccio AR, Valinsky J, et al. Stem cell factor induces proliferation and differentiation of highly enriched murine hematopoietic cells. Proc Natl Acad Sci U S A 1991;88:7420–4.
20. Dolci S, Williams DE, Ernst MK, et al. Requirement for mast cell growth factor for primordial germ cell survival in culture. Nature 1991;352:809–11.
21. Tsai M, Shih LS, Newlands GF, et al. The rat c-kit

ligand, stem cell factor, induces the development of connective tissue-type and mucosal mast cells *in vivo*. Analysis by anatomical distribution, histochemistry, and protease phenotype. J Exp Med 1991; 174:125–31.

22. Huizinga JD, Thuneberg L, Kluppel M, Malysz J, Mikkelsen HB, Bernstein A. W/kit gene required for interstitial cells of Cajal and for intestinal pacemaker activity. Nature 1995;373:347–9.

23. Hirota S, Isozaki K, Moriyama Y, et al. Gain-of-function mutations of c-kit in human gastrointestinal stromal tumors. Science 1998;279:577–80.

24. Medeiros F, Corless CL, Duensing A, et al. KIT-negative gastrointestinal stromal tumors: proof of concept and therapeutic implications. Am J Surg Pathol 2004;28:889–94.

25. Heinrich MC, Corless CL, Duensing A, et al. PDGFRA activating mutations in gastrointestinal stromal tumors. Science 2003;299:708–10.

26. Buchdunger E, Cioffi CL, Law N, et al. Abl protein-tyrosine kinase inhibitor STI571 inhibits *in vitro* signal transduction mediated by c-kit and platelet-derived growth factor receptors. J Pharmacol Exp Ther 2000; 295:139–45.

27. Druker BJ. Inhibition of the Bcr-Abl tyrosine kinase as a therapeutic strategy for CML. Oncogene 2002; 21:8541–6.

28. Druker BJ. STI571 (Gleevec) as a paradigm for cancer therapy. Trends Mol Med 2002;8:S14–8.

29. von Mehren M, Blanke CD, Joensuu H, et al. High incidence of durable responses induced by Imatinib Mesylate (GleevecTM) in patients with unresectable and metastatic gastrointestinal stromal tumors (GISTs). In: The American Society of Clinical Oncology, editors. Orlando (FL); 2002. p. a1608.

30. Heinrich MC, Corless CL, Demetri GD, et al. Kinase mutations and imatinib response in patients with metastatic gastrointestinal stromal tumor. J Clin Oncol 2003;21:4342–9.

31. Debiec-Rychter M, Dumez H, Judson I, et al. Use of c-KIT/PDGFRA mutational analysis to predict the clinical response to imatinib in patients with advanced gastrointestinal stromal tumours entered on phase I and II studies of the EORTC Soft Tissue and Bone Sarcoma Group. Eur J Cancer 2004;40:689–95.

32. Mol CD, Dougan DR, Schneider TR, et al. Structural basis for the autoinhibition and STI-571 inhibition of c-Kit tyrosine kinase. J Biol Chem 2004;279: 31655–63.

33. Canutescu AA, Shelenkov AA, Dunbrack RL Jr. A graph-theory algorithm for rapid protein side-chain prediction. Protein Sci 2003;12:2001–14.

34. Huang CC, Couch GS, Pettersen EF, Ferrin TE. Chimera: an extensible molecular modeling application constructed using standard components. In: Pacific Symposium on Biocomputing. 1996. p. 724.

35. Fletcher CD, Berman JJ, Corless C, et al. Diagnosis of gastrointestinal stromal tumors: a consensus approach. Int J Surg Pathol 2002;10:81–9.

36. Corless CL, Fletcher JA, Heinrich MC. Biology of gastrointestinal stromal tumors. J Clin Oncol 2004;22: 3813–25.

37. Lasota J, Wozniak A, Sarlomo-Rikala M, et al. Mutations in exons 9 and 13 of KIT gene are rare events in gastrointestinal stromal tumors. A study of 200 cases. Am J Pathol 2000;157:1091–5.

38. Kinoshita K, Isozaki K, Hirota S, et al. c-kit gene mutation at exon 17 or 13 is very rare in sporadic gastrointestinal stromal tumors. J Gastroenterol Hepatol 2003;18:147–51.

39. Kim TW, Lee H, Kang YK, et al. Prognostic significance of c-kit mutation in localized gastrointestinal stromal tumors. Clin Cancer Res 2004;10: 3076–81.

40. Hou YY, Tan YS, Sun MH, et al. C-kit gene mutation in human gastrointestinal stromal tumors. World J Gastroenterol 2004;10:1310–4.

41. Demetri GD. Identification and treatment of chemoresistant inoperable or metastatic GIST: experience with the selective tyrosine kinase inhibitor imatinib mesylate (STI571). Eur J Cancer 2002;38 Suppl 5: S52–9.

42. Demetri GD, von Mehren M, Blanke CD, et al. Efficacy and safety of imatinib mesylate in advanced gastrointestinal stromal tumors. N Engl J Med 2002;347: 472–80.

43. Eisenberg BL, von Mehren M. Pharmacotherapy of gastrointestinal stromal tumours. Expert Opin Pharmacother 2003;4:869–74.

44. Eisenberg BL. Imatinib mesylate: a molecularly targeted therapy for gastrointestinal stromal tumors. Oncology (Huntingt) 2003;17:1615–20; discussion 20, 23, 26 passim.

45. von Mehren M. Recent advances in the management of gastrointestinal stromal tumors. Curr Oncol Rep 2003;5:288–94.

46. von Mehren M. Gastrointestinal stromal tumors: a paradigm for molecularly targeted therapy. Cancer Invest 2003;21:553–63.

47. Heinrich MC, Blanke CD, Druker BJ, Corless CL. Inhibition of KIT tyrosine kinase activity: a novel molecular approach to the treatment of KIT-positive malignancies. J Clin Oncol 2002;20:1692–703.

48. Heinrich MC, Rubin BP, Longley BJ, Fletcher JA. Biology and genetic aspects of gastrointestinal stromal tumors: KIT activation and cytogenetic alterations. Hum Pathol 2002;33:484–95.

49. Paez JG, Janne PA, Lee JC, et al. EGFR mutations in lung cancer: correlation with clinical response to gefitinib therapy. Science 2004;304:1497–500.

50. Sordella R, Bell DW, Haber DA, Settleman J. Gefitinib-sensitizing EGFR mutations in lung cancer activate anti-apoptotic pathways. Science 2004; 305:1163–7.

51. Miettinen M, Sarlomo-Rikala M, Lasota J. Gastrointestinal stromal tumors: recent advances in understanding of their biology. Hum Pathol 1999;30:1213–20.

52. Nishida T, Hirota S, Taniguchi M, et al. Familial gastrointestinal stromal tumours with germline mutation of the KIT gene. Nat Genet 1998;19:323–4.

53. Maeyama H, Hidaka E, Ota H, et al. Familial gastrointestinal stromal tumor with hyperpigmentation: association with a germline mutation of the c-kit gene. Gastroenterology 2001;120:210–5.

54. Isozaki K, Terris B, Belghiti J, Schiffmann S, Hirota S, Vanderwinden JM. Germline-activating mutation in the kinase domain of KIT gene in familial gastrointestinal stromal tumors. Am J Pathol 2000;157:1581–5.

55. Hirota S, Nishida T, Isozaki K, et al. Familial gastrointestinal stromal tumors associated with dysphagia and novel type germline mutation of KIT gene. Gastroenterology 2002;122:1493–9.

56. Robson ME, Glogowski E, Sommer G, et al. Pleomorphic characteristics of a germ-line KIT mutation in a large kindred with gastrointestinal stromal tumors, hyperpigmentation, and dysphagia. Clin Cancer Res 2004;10:1250–4.

57. Chan PM, Ilangumaran S, La Rose J, Chakrabartty A, Rottapel R. Autoinhibition of the kit receptor tyrosine kinase by the cytosolic juxtamembrane region. Mol Cell Biol 2003;23:3067–78.

58. Ma Y, Cunningham ME, Wang X, Ghosh I, Regan L, Longley BJ. Inhibition of spontaneous receptor phosphorylation by residues in a putative α-helix in the KIT intracellular juxtamembrane region. J Biol Chem 1999;274:13399–402.

59. Ma Y, Longley BJ, Wang X, Blount JL, Langley K, Caughey GH. Clustering of activating mutations in c-KIT's juxtamembrane coding region in canine mast cell neoplasms. J Invest Dermatol 1999;112:165–70.

60. Samuels Y, Velculescu VE. Oncogenic mutations of PIK3CA in human cancers. Cell Cycle 2004;3:1221–4.

61. Broderick DK, Di C, Parrett TJ, et al. Mutations of PIK3CA in anaplastic oligodendrogliomas, high-grade astrocytomas, and medulloblastomas. Cancer Res 2004;64:5048–50.

62. Bachman KE, Argani P, Samuels Y, et al. The PIK3CA gene is mutated with high frequency in human breast cancers. Cancer Biol Ther 2004;3:772–5.

63. Samuels Y, Wang Z, Bardelli A, et al. High frequency of mutations of the PIK3CA gene in human cancers. Science 2004;304:554.